

Anti-Oil-fouling Superhydrophilic Composite Aerogel for

Solar Saline Alkali Water Desalination

Jiayu Yan, Zhen Zhang, Yongxin Shi, Qinglai Che, Qing Miao, Guihua Meng*, Zhiyong Liu*

School of Chemistry and Chemical Engineering, Shihezi University/Key Laboratory for Green Processing of Chemical Engineering of Xinjiang Bingtuan/Key Laboratory of Materials-Oriented Chemical Engineering of Xinjiang Uygur Autonomous Region/Engineering Research Center of Materials-Oriented Chemical Engineering of Xinjiang Bingtuan, Shihezi, Xinjiang 832003, P.R. China

***Corresponding author:** Dr. Guihua Meng & Prof. Zhiyong Liu

School of Chemistry and Chemical Engineering/Key Laboratory for Green Processing of Chemical Engineering of Xinjiang Bingtuan, Xinjiang, P.R. China, 832003

Address: Beisi Road, Shihezi City, Xinjiang, 832003, P.R. China

E-mail Address: mghua0726@sina.com, lzyongclin@sina.com

Contents

S1. Photo of the ASG-0PANi aerogel (white) and ASG aerogel (black).

S2. The local zoomed-in Images show the water-absorbing capacity of the ASG aerogel.

S3. Analysis of mercury-pressing data of ASG-0PANi and ASG aerogel.

Table S1. Porosity of ASG samples.

Table S2. Detailed parameters for calculating solar thermal efficiency of ASG samples under one-sun illumination.

Table S3. Detailed parameters for calculating solar thermal efficiency of water, ASG-0PANI, ASG and ASG-0SA aerogel under one-sun illumination

S4. The stress-strain curves of ASG aerogel at compressive strain.

S5. Schematic of the ASG aerogel solar-driven interfacial evaporation device.

S6. Photos of ASG aerogel floating on the water surface at different heights and top-view.

S7. Evaporation mass loss for different thickness of ASG aerogel under one-sun illumination for 1 h.

S8. Evaporation mass loss for different aniline monomer concentrations of ASG aerogel under one-sun illumination for 1 h.

S9. Linear dependency of salinity and conductance of NaCl solution under 25 °C.

Table S4. Comparison parameters for a solar steam generation made with different kinds of materials.



Figure S1. Photo of the ASG-0PANi aerogel (white) and ASG aerogel (black).

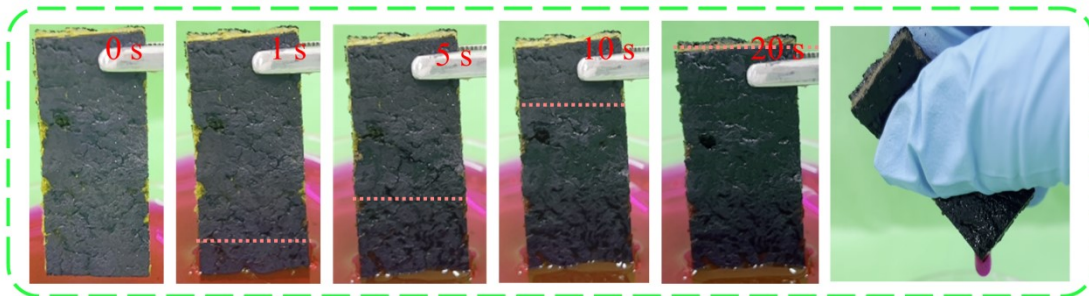


Figure S2. The local zoomed-in Images show the water-absorbing capacity of the ASG aerogel.

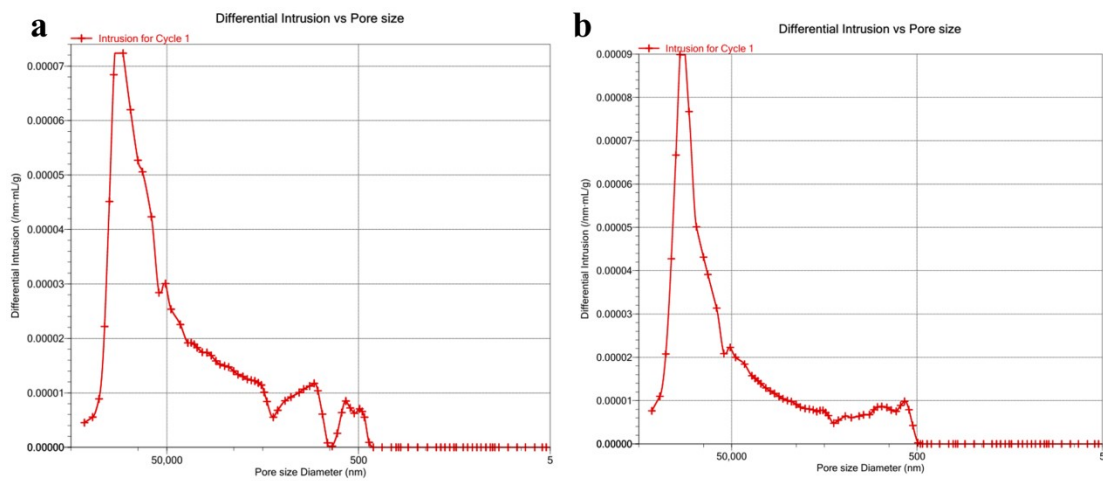


Figure S3. Analysis of mercury-pressing data of ASG-0PANi and ASG aerogel.

Table S1. Porosity of ASG samples.

Samples	Porosity (%)	Bulk density (g/mL)	Average pore size (nm)	Total hole capacity(mL/g)	Total hole area(m ² /g)
ASG-0PANi aerogel	93.11	0.0700	102761.25	13.3070	0.518
ASG aerogel	93.35	0.0798	93412.72	11.6965	0.561

Table S2. Detailed parameters for calculating solar thermal efficiency

Samples	Water mass loss rate (Kg h ⁻² h-1)	Average water temperature difference (°C)	Sensible heat (J Kg ⁻¹)	Latent heat (J Kg ⁻¹)	η (%)
ASG-0.02	0.91	15.3	64.26		55.4
ASG-0.05	1.46	19.8	83.16		91.5
ASG-0.10	1.19	17.7	74.34	2260	73.8
ASG-0.15	0.89	19.2	80.64		54.1
ASG-0.20	0.85	19.4	81.48		51.8

Table S3. Detailed parameters for calculating solar thermal efficiency

Samples	Water mass loss rate (Kg h ⁻² h-1)	Average water temperature difference (°C)	Sensible heat (J Kg ⁻¹)	Latent heat (J Kg ⁻¹)	η (%)
Blank water	0.41	10.9	45.78		22.8
ASG-0PANi aerogel	0.67	14.6	61.32		39.7
ASG-0SA aerogel	1.14	17.9	75.18	2260	70.8
ASG aerogel	1.46	19.8	83.16		91.5

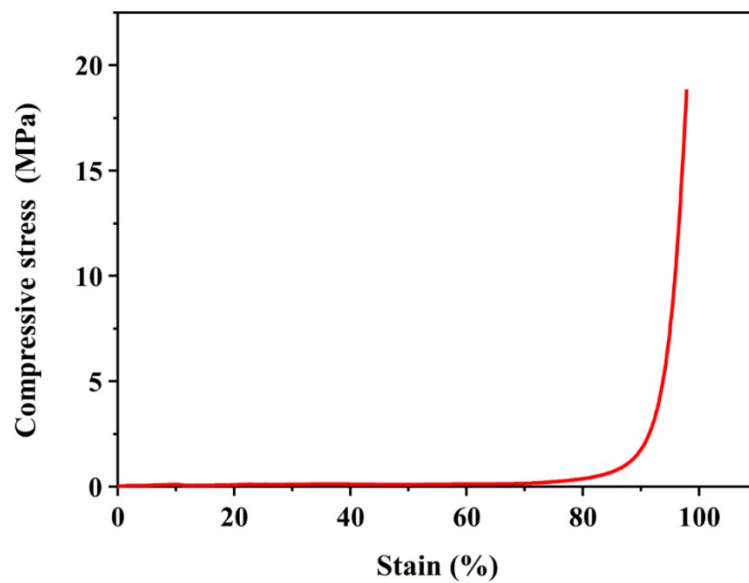


Figure S4. The stress-strain curves of ASG aerogel at compressive strain.

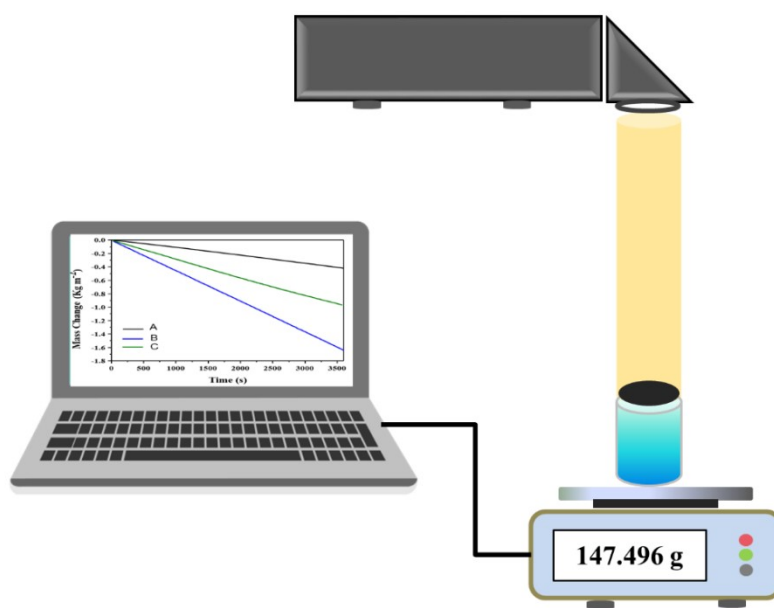


Figure S5. Schematic of the ASG aerogel solar-driven interfacial evaporation device

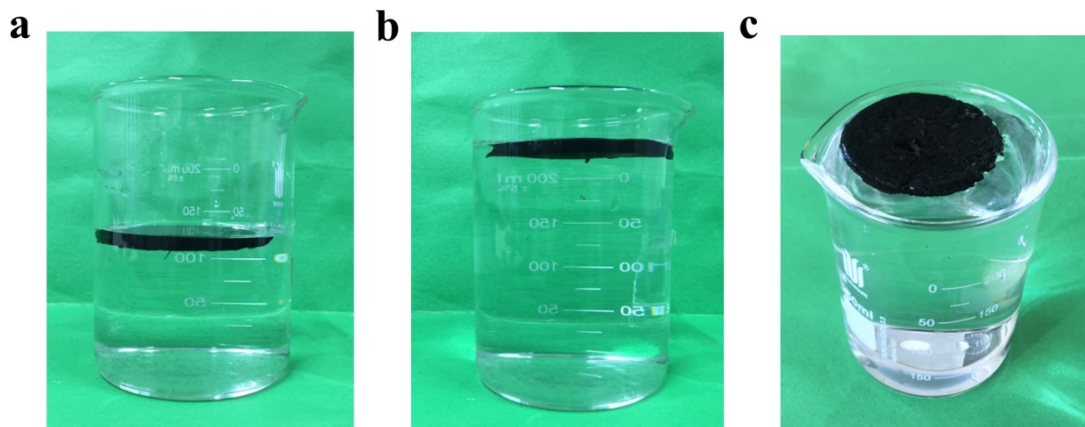


Figure S6. Photos of ASG aerogel floating on the water surface at different heights and top-view, the water was then pumped up and diffused to the entire surface of the PVA/SA/PANi aerogel by hydrophilic interaction.

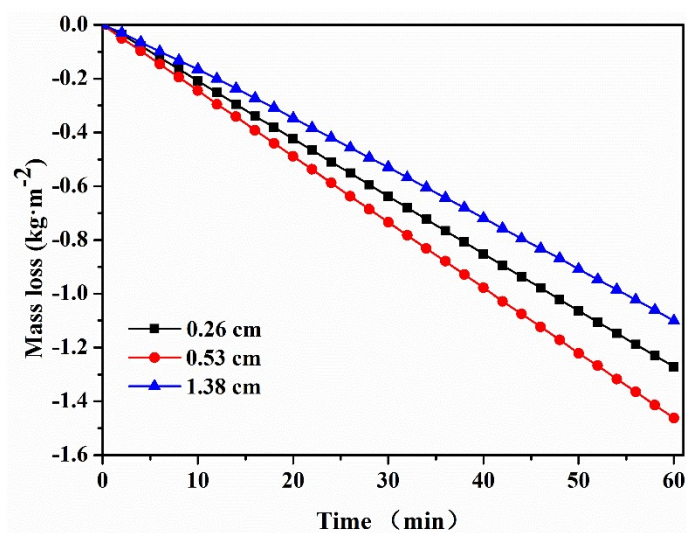


Figure S7. Evaporation mass loss for different thickness of ASG aerogel under one-sun illumination for 1 h.

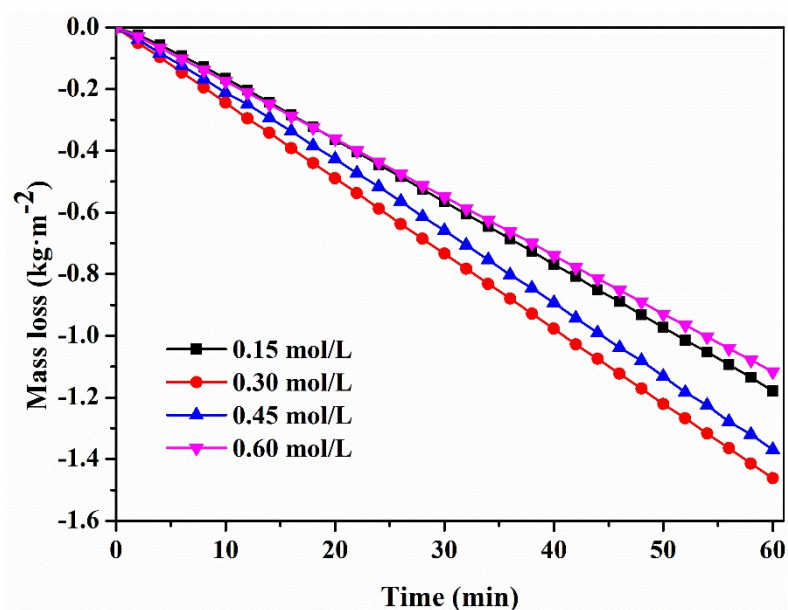


Figure S8. Evaporation mass loss for different aniline monomer concentrations of ASG aerogel under one-sun illumination for 1 h.

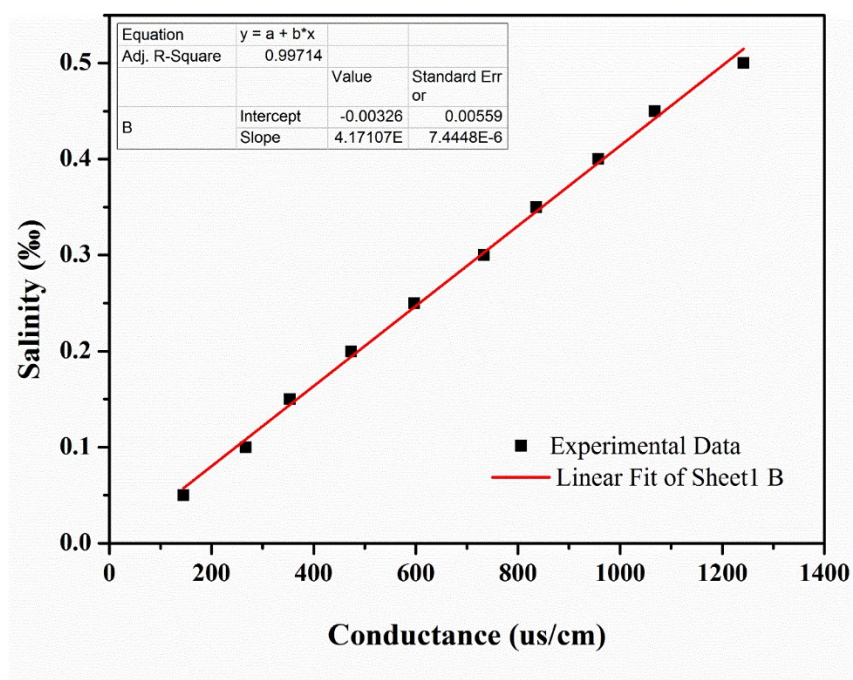


Figure S9. Linear dependency of salinity and conductance of NaCl solution under 25 °C.

The salinity and conductance of the NaCl solution exhibited a linear dependency in a range of salinity from 0.05 to 0.5 ‰. The standard curve was established for the calculation of salinity of purified water from artificial brine water. Three brine samples with representative simulated salinities (g dissolved salt / kg seawater, i.e. ‰), mild (lowest salinity 1.31 ‰), moderate (average salinity 5.22 ‰), and severe (highest salinity 13.10 ‰), were used and

carefully tracked by a conductivity test.

Table S4 Comparison parameters for a solar steam generation made with different kinds of materials.

Materials	Solar absorbers	Efficiency %	Evaporation rate $\text{kg} \cdot \text{m}^{-2} \cdot \text{h}^{-1}$	Reference
Aerogel	PANi	94.0%	1.65	Ref. ¹
Carbon fiber	PANi	93.7%	1.43	Ref. ²
Hydrogel	PANi	91.5%	1.40	Ref. ³
Aerogel	PANi	91.5%	1.46	This work
MOFs	PANi	90.8%	1.87	Ref. ⁴
Aerogel	PANi	90.0%	1.58	Ref. ⁵
Fabric	PANi	89.9%	1.94	Ref. ⁶
Foam	PANi	87.3%	1.50	Ref. ⁷
Cotton	bSno@PANi	87.0%	1.74	Ref. ⁸
Membrane	PANi	85.0%	1.41	Ref. ⁹
Foam	PANi	80.5%	1.17	Ref. ¹⁰
Membrane	PANi	74.2%	1.09	Ref. ¹¹

1. S. Li, Y. Y. He, Y. N. Wang, D. G. Liao, H. X. Liu, L. Zhou, C. Wei, C. B. Yu and Y. H. Chen, *Macromol. Mater. Eng.*, 2021, **306**.
2. K. Wang, B. B. Huo, F. Liu, Y. W. Zheng, M. H. Zhang, L. Cui and J. Q. Liu, *Desalination*, 2020, **481**.
3. X. Yin, Y. Zhang, Q. Guo, X. Cai, J. Xiao, Z. Ding and J. Yang, *ACS Appl Mater Interfaces*, 2018, **10**, 10998-11007.
4. Z. Li, X. Ma, D. Chen, X. Wan, X. Wang, Z. Fang and X. Peng, *Adv. Sci.*, 2021, **8**, 2004552.
5. S. Li, Y. Y. He, Y. P. Guan, X. Y. Liu, H. X. Liu, M. S. Xie, L. Zhou, C. Wei, C. B. Yu and Y.

- H. Chen, *Acs Applied Polymer Materials*, 2020, **2**, 4581-4591.
6. Z. X. Liu, B. H. Wu, B. Zhu, Z. G. Chen, M. F. Zhu and X. G. Liu, *Advanced Functional Materials*, 2019, **29**, 1905485.
 7. K. Wang, Z. Cheng, P. Li, Y. Zheng, Z. Liu, L. Cui, J. Xu and J. Liu, *J. Colloid Interface Sci.*, 2021, **581**, 504-513.
 8. N. Sharma, N. Swaminathan, C. H. Chi, R. B. Gurung and H. F. Wu, *Journal of Industrial and Engineering Chemistry*, 2022, **107**, 45-52.
 9. Y. Zou, X. F. Chen, W. C. Guo, X. H. Liu and Y. W. Li, *Acs Applied Energy Materials*, 2020, **3**, 2634-2642.
 10. Q. Chen, Z. Pei, Y. Xu, Z. Li, Y. Yang, Y. Wei and Y. Ji, *Chem Sci*, 2018, **9**, 623-628.
 11. Y. Peng, Y. Wang, W. Li and J. Jin, *Journal of Materials Chemistry A*, 2021, **9**, 10678-10684.